

Photoemission study of Kr $3d \rightarrow np$ autoionization resonances

D. W. Lindle,* P. A. Heimann, T. A. Ferrett,* M. N. Piancastelli,[†] and D. A. Shirley

*Materials and Molecular Research Division, Lawrence Berkeley Laboratory,
and Department of Chemistry, University of California, Berkeley, California 94720*

(Received 27 January 1987)

Resonant photoelectron spectra of Kr have been taken in the photon-energy ranges of the $3d_{5/2} \rightarrow 5p, 6p$ and $3d_{3/2} \rightarrow 5p$ excitations. The spectra, which closely resemble normal $Kr^+ 3d^{-1}$ Auger spectra, illustrate the importance of "spectator" Auger-like decay for inner-shell resonances, in which the initially excited electron does not participate in the core-hole deexcitation process, except to respond to the change in the atomic potential. Possible assignments for some of the spectator decay channels are discussed based on photoemission intensity measurements at the different $3d$ resonances. These assignments suggest that shake-up (e.g., $5p \rightarrow 6p$) of the "spectator" electron during the decay process is not quite as important as previously suspected. The resonance profiles of some of the more intense satellites have been determined over the $3d \rightarrow np$ resonances. Very small resonance effects also were observed in the partial cross section for $4p$ subshell ionization, which produced asymmetric Fano-type profiles. The $4p$ angular distribution, in contrast, exhibits a pronounced effect in the resonance energy range. The $4p$ results demonstrate that nonspectator autoionization also is present.

I. INTRODUCTION

Photoemission decay characteristics of inner-shell discrete resonances in atoms have been studied recently in a few systems.¹⁻¹⁰ For excitations to Rydberg states leading to an inner-subshell threshold, the resulting photoelectron spectrum generally exhibit peaks associated with decay channels in which the electron initially excited to the Rydberg orbital remains as a "spectator electron" to the decay process.^{8,9} The final ionic states thus produced correspond to photoemission satellites. Also, the resonant photoelectron spectra appear similar to the "normal" Auger spectrum that one obtains with photon energies above the ionization threshold. For example, excitation of a $4d$ electron in Xe to a $6p$ orbital can result in a Xe^+ ion with the configuration $4d^{10}5p^46p$,^{1-4,6,8} where the electron excited to the $6p$ orbital can be considered to have remained there while two $5p$ electrons interacted to fill the $4d$ hole. This description in terms of Auger-like decay also suffices to explain the resemblance between the resonant photoemission spectrum and the above-threshold Auger spectrum.

These qualitative arguments also apply to the Kr $3d \rightarrow np$ excitations studies in this work. The Kr resonance spectra^{1,7} resemble the $3d^{-1}$ Auger-decay spectrum,^{7,11-13} and this similarity has been used to assign some of the resonance decay channels.^{1,7} However, this spectator-electron picture for inner-shell resonance decay is oversimplified, and differences from the Auger spectrum have been observed. Because the discrete excitations involve only one spin-orbit state (e.g., $3d_{5/2} \rightarrow 5p$), the resonance spectra should show fewer peaks than the $M_{4,5}NN$ Auger spectrum. On the other hand, evidence suggests^{1,7,10} that there is an enhanced probability, relative to $3d^{-1}$ Auger decay, for an electron initially excited into the $5p$ orbital to be further excited to a higher-lying orbi-

tal (e.g., $6p$) or into the continuum during the deexcitation process of the $3d \rightarrow np$ resonances. This effect would create more peaks with appreciable intensity in the resonance spectra. Finally, because of the presence of the np electron in the Kr^+ final state, the energies of the photoelectrons emitted on resonance are shifted by ~ 5 eV to higher kinetic energy with respect to $M_{4,5}NN$ Auger electrons. It is clear that the spectator model should include these effects, and we discuss our results in this more comprehensive picture. All of these effects have been observed previously,^{1,7,10} as well as in the Kr $3d$ resonance spectra reported here. In addition, by exciting the $3d$ electron to different orbitals (i.e., $5p$ or $6p$), we observed the enhancement of different decay channels, and we have used this information to suggest new assignments for a few of the spectator satellites.

Nonspectator autoionization decay also can occur for inner-shell resonances, although generally it is less intense than spectator decay.⁸ By nonspectator decay in Kr, we mean transitions which result in either $Kr^+(4p)$ or $Kr^+(4s)$. While no resonant effect on the $4s$ photoemission channel could be observed in this experiment, we did find that the $4p$ partial cross section exhibits small effects, with asymmetric profiles, over the $3d \rightarrow np$ resonances. Furthermore, the $4p$ angular distribution is markedly affected in the resonance region. These data illustrate a breakdown of the spectator model in describing atomic inner-shell resonances, and indicate that the valence main-line photoemission channels can couple significantly to core-level excitations.

The experimental technique is reviewed in Sec. II. Section III contains a discussion of the resonant photoemission spectra as well as a presentation of the resonance profiles for the cross sections of some of the spectator satellites, and for the $4p$ cross section and asymmetry parameter. Conclusions are presented in Sec. IV.

II. EXPERIMENTAL PROCEDURE

The experiment was performed on the new "grasshopper" monochromator at the Stanford Synchrotron Radiation Laboratory with the time-of-flight (TOF) apparatus¹⁴ used in previous inner-shell studies of the rare gases.^{4,15,16} The experimental conditions were the same as described in these earlier measurements, with the exception that the monochromator resolution was 0.10 eV (0.15 Å) for the Kr $3d \rightarrow np$ resonance spectra.

The differential cross section for gas-phase photoemission in the dipole approximation is given by¹⁷

$$\frac{d\sigma(h\nu, \theta)}{d\Omega} = \frac{\sigma(h\nu)}{4\pi} [1 + \beta(h\nu)P_2(\cos\theta)], \quad (1)$$

where θ is the angle between the photon polarization and the direction of electron emission, $\sigma(h\nu)$ and $\beta(h\nu)$ are the photoionization cross section and angular-distribution asymmetry parameter for the ionization process being studied, and $P_2(\cos\theta)$ is the second Legendre polynomial. With the TOF apparatus,^{4,15,16} cross sections are determined with one analyzer situated at $\theta=54.7^\circ$. A second analyzer at $\theta=0^\circ$ is included to allow simultaneous measurement of asymmetry parameters.

For the Kr measurements, the electron-energy resolution was improved by applying a retarding voltage of 20 V over a portion of the photoelectrons' flight path. Unfortunately, this also caused the analyzer transmission to drop by a factor of 2 from 70 to 30 eV kinetic energy. The spectra shown in Fig. 1 are not corrected for this changing transmission, but the cross sections reported in Table I and shown in Figs. 2–5 have been corrected. As in previous experiments, we estimate systematic errors to be approximately $\pm 10\%$ for cross sections and ± 0.1 for asymmetry parameters.

III. RESULTS AND DISCUSSION

We begin this section by presenting photoemission spectra taken on the $3d_{5/2} \rightarrow 5p, 6p$ and $3d_{3/2} \rightarrow 5p$ resonances (91.20, 92.42, and 92.56 eV, respectively¹⁸). Section III A includes a discussion of these spectra, the previous assignments of some of the resonantly enhanced peaks, and a few newly suggested assignments based on the present higher photon-energy-resolution measurements. In Sec. III B, we present resonance profiles for the cross sections of the more-intense and better-resolved spectator transitions. Also included in this section are resonance profiles for the $4p$ cross section and asymmetry parameter.

A. Resonance photoemission spectra

Resonance TOF photoemission spectra are presented in Fig. 1 for the $3d_{5/2} \rightarrow 5p, 6p$ and $3d_{3/2} \rightarrow 5p$ resonances, compared with an off-resonance spectrum taken at 89.9-eV photon energy. These spectra have not been corrected for the changing analyzer transmission, so that peak 8 is too small by a factor of 2 relative to the high-energy peaks. At 89.9 eV, we see only the $4s$ and $4p$ main lines, and the $3d$ main line and $3d^{-1}M_{4,5}N_{2,3}N_{2,3}$ Auger lines. The latter two features are due to second-order radiation. The $3d^{-1}$ Auger feature in the 89.9-eV spectrum prob-

ably also has contributions from photoemission satellites of the $4s$ and $4p$ lines due to the primary photon energy. Figure 1 illustrates that there are no peaks due to second-order radiation which interfere with the resonantly enhanced peaks in the other three spectra, with the exception of peak 1a, which includes a small constant background intensity. The peak labels are taken from Aksela *et al.*,⁷ and assignments given in Ref. 7 are included in Table I.

Considering the 91.2-eV spectrum in Fig. 1, we see by comparison with the 89.9-eV spectrum that the $4s$ and $4p$ lines are affected very little by $3d_{5/2} \rightarrow 5p$ autoionization, while many other photoemission lines are produced on resonance. The assignments and peak cross sections (corrected for analyzer transmission) of the features in the 91.2-eV spectrum are given in Table I. Also included in Table I is the relative resonant intensity for each peak,

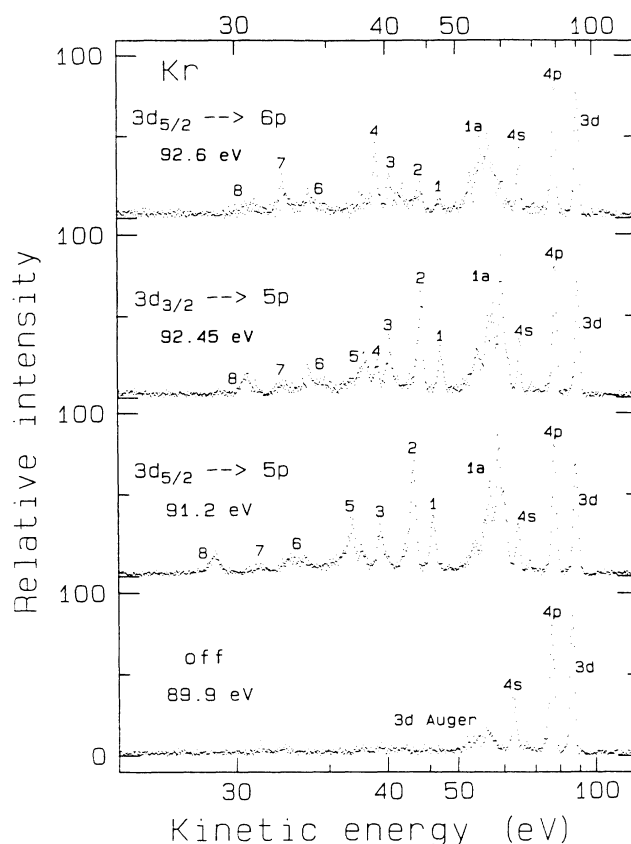


FIG. 1. Resonant TOF photoelectron spectra of Kr at 89.9-, 91.2-, 92.45-, and 92.6-eV photon energy, which correspond to off-resonance excitation, and excitation of the $3d_{5/2} \rightarrow 5p$, $3d_{3/2} \rightarrow 5p$, and $3d_{5/2} \rightarrow 6p$ resonances, respectively. The spectra are not corrected for analyzer transmission, which varies monotonically from 0.5 to 1 between 30- and 70-eV kinetic energy. The spectra have been scaled so that relative peak intensities in different spectra can be compared. The peak labels are from Ref. 7. The $3d$ peak is produced by second-order radiation, and the $3d$ Auger peak in the 89.9-eV spectrum is the $M_{4,5}N_{2,3}N_{2,3}$ Auger from the decay of these "second-order" $3d$ -hole states. The $3d$ Auger peak also has a small contribution from valence satellites.

TABLE I. Assignments of the photoemission decay channels of Kr $3d \rightarrow np$ resonances, and their relative intensities and kinetic energies at the $3d_{5/2} \rightarrow 5p$ resonance.

| Peak | Assignment | | $3d_{5/2} \rightarrow 5p$ resonance | | Kinetic energy (eV) ^c |
|-----------|-----------------------------------|--|-------------------------------------|---|----------------------------------|
| | Aksela <i>et al.</i> ^a | Present | Peak cross section (Mb) | Relative enhancement (peak 1a = 100) ^b | |
| $4p^{-1}$ | | | 0.37(1) | 3 | 77.1(3) |
| $4s^{-1}$ | | | 0.13(1) | | 63.7(3) |
| 1a | $4p^4 5p$, $4p^4 6p$, etc. | | 1.47(3) | 100 | 52.6–61.0 |
| 1 | $4s4p^5(^1P)5p$ | | 0.28(1) | 19 | 45.8(2) |
| 2 | $4s4p^5(^3P)5p$ | | 0.58(2) | 39 | 43.1(2) |
| 3 | $4s4p^5 6p$ | | 0.27(1) | 18 | 39.3(2) |
| 4 | | $4s4p^5 6p$, $4s4p^5 7p$ | v.w. ^d | < 1 | 37.9(3) |
| 5 | $4p^3 4d 5p$ | | 0.55(2) | 37 | 36.8(2) |
| 6 | $4p^3 4d 6p$ | $4p^3 4d 5p$, $4p^3 4d 6p$, $4p^3 4d 7p$ | 0.23(2) | 16 | 33.3(3) 32.5(3) |
| 7 | | $4p^3 4d 6p$, $4p^3 4d 7p$ | v.w. ^d | < 1 | 31.1(3) |
| 8 | $4s^0 5p$ | | 0.26(3) | 18 | 29.1(2) |

^aReference 7.

^bIncludes only resonant enhancement of $4p$ (10%) and $4s$ (0%).

^cAdd 1.2 eV for $3d_{3/2} \rightarrow 5p$.

^dVery weak.

with peak 1a set to 100. For peak 1a and the $4s$ and $4p$ lines, the reported relative intensity includes only the resonant enhancement, because the nonresonant intensity has been subtracted. From these values, we find that much of the resonance decay to Kr^+ is via spectator transitions. Of the Kr^+ spectator satellites, the configurations $4p^4 5p$ and $4s4p^5 5p$ are the most important, as expected by considering the resonant decay as being similar to $3d^{-1}$ Auger decay. Also significant is the configuration $4p^3 4d 5p$, which arises from configuration interaction with $4s4p^5 5p$.⁷

The kinetic energies and relative intensities of the features in the 91.2-eV spectrum reported here agree well with previous measurements.⁷ One exception is that Aksela *et al.*⁷ observed peaks 4 and 7 to be nearly as large as peak 3 at 91.2-eV photon energy. In Fig. 1, peaks 4 and 7 are very small. We believe this discrepancy arises because the previous work had more second-order contributions (from Kr^+ $M_{4,5}NN$ Auger) to the resonant spectra as discussed in Ref. 7. Comparing the resonant spectra to Kr^+ Auger spectra,^{7,11–13} peaks 4 and 7 occur at the same energy as the most intense $M_{4,5}N_1N_{2,3}$ Auger features, consistent with second-order contamination being a likely explanation for the differences between the two experiments. As noted previously, there are no discernible second-order Kr^+ Auger peaks in our spectra, as can be seen in the off-resonance 89.9-eV spectrum resonance 89.9-eV spectrum in Fig. 1.

Comparing the $3d_{5/2} \rightarrow 5p$ (91.2 eV) and $3d_{3/2} \rightarrow 5p$ (92.45 eV) photoelectron spectra in Fig. 1, the overall peak structures are very similar, with a shift to higher energy of 1.2 eV for the latter spectrum because of the higher photon energy. Peaks 4 and 7 and possibly the low-energy

side of peak 6, however, are larger in the $3d_{3/2} \rightarrow 5p$ spectrum. This observation can be explained by considering the 92.6-eV spectrum, which primarily represents the $3d_{5/2} \rightarrow 6p$ excitation. The $3d_{3/2} \rightarrow 5p$ and $3d_{5/2} \rightarrow 6p$ resonances are separated by only 0.1 eV, and thus we expect photoemission decay features from both resonances to appear in each spectrum, with varying intensities depending on the photon energy. Indeed, the relatively enhanced peaks in the 92.6 eV spectrum ($3d_{5/2} \rightarrow 6p$) are 4, 6 (low-energy side only), and 7, exactly the same peaks which are stronger in the $3d_{3/2} \rightarrow 5p$ spectrum in comparison to the $3d_{5/2} \rightarrow 5p$ spectrum.

This enhancement of only peaks 4, 6, and 7 on the $3d_{5/2} \rightarrow 6p$ resonance suggests that these peaks have contributions from Kr^+ configurations containing a $6p$ spectator electron. However, there is evidence¹⁹ that the corresponding resonance in Xe (i.e., $4d_{5/2} \rightarrow 7p$) decays with the $7p$ electron being shaken-up to the $8p$ orbital more often than remaining in the $7p$ orbital. Therefore, it is possible that these enhanced peaks (4, 6, and 7) in the Kr $3d_{5/2} \rightarrow 6p$ spectrum correspond to configurations with a $7p$ electron, instead of a $6p$ electron. Based on our observation, we assign peaks 4 and 7 to the $4s4p^5 np$ and $4p^3 4d np$ Kr^+ configurations, where n can be 6 or 7. It also seems likely that peak 6 has a contribution from a different multiplet of the $4p^3 4d np$ ($n = 6$ or 7) configuration (low-energy side), as well as from the $4p^3 4d 5p$ configuration (high-energy side). These new assignments are given in Table I along with the assignments of Aksela *et al.*,⁷ who previously assigned $4s5p^5 6p$ and $4p^3 4d 6p$ configurations to peaks 3 and 6. Their assignment for peak 3 suggests that the 92.6-eV spectrum should show some enhancement of feature 3. In fact, comparison of

peak 3 to peaks 1 and 2 in the top of Fig. 1 demonstrates a slight relative enhancement of peak 3, confirming at least partially the assignment of Ref. 7.

The remaining assignments by Aksela *et al.*⁷ of peaks 1a, 1, 2, 5, and 8 to configurations with 5*p* spectator electrons is supported by our observation that the intensity of these peaks is reduced at the $3d_{5/2} \rightarrow 6p$ resonance, as would be expected in the spectator-satellite picture. The fact that peak 1a remains relatively strong at 92.6 eV probably results from the presence of $4p^6 6p$ configurations in this peak.⁷ Additional evidence of the presence of $4p^4 6p$ configurations in peak 1a is provided by comparison of the kinetic-energy distribution of peak 1a in the 92.45- and 92.6-eV spectra. On the $3d_{5/2} \rightarrow 6p$ resonance, the intensity of peak 1a has shifted to lower kinetic energy presumably because of the relative enhancement of the higher-binding-energy $4p^4 6p$ states.

Finally, the assignments for peaks 1–7 indicate the shake-up of the 5*p* electron to the 6*p* orbital during the Auger-like decay process is not quite as important as suggested previously.^{1,7} We estimate that this shake-up intensity is $\sim 20\%$ of the intensity of final states where the 5*p* electron remains in the 5*p* orbital. Previous workers found it to be near 30%,⁷ or even larger.¹ The rather low fraction of resonant shake-up decay observed here is perhaps surprising, because recent threshold-electron measurements¹⁰ have found that the Kr $3d \rightarrow np$ resonances decay appreciably [37(8)%] to double-ionization channels, often by “shaking off” the 5*p* electron. Because shake-off appears to be an important decay path for these inner-shell resonances, one might expect shake-up to be more intense as well.

In summary, we find reasonable agreement with earlier photoemission results for the Kr $3d \rightarrow 5p$ resonances. The dominance of spectator-satellite decay over main-line autoionization for these excitations is confirmed. By preferentially exciting the $3d_{5/2} \rightarrow 6p$ resonance, we have been able to assign features in the resonant spectra to configurations containing a 6*p* or 7*p* electron. These new assignments show that $5p \rightarrow 6p$ shake-up during resonant Auger-like decay of the Kr $3d \rightarrow 5p$ excitations is not as important as believed earlier, although more detailed measurements and calculations of the final-state transition probabilities are needed to confirm this finding.

B. Resonance profiles

For the more intense spectator-transition satellites in Fig. 1 (1a, 1, and 2), we were able to measure the resonance profiles through the $3d \rightarrow np$ region. We show in Figs. 2–4 the cross sections for the $4p^4 np$, $4s4p^5(^1P)5p$, and $4s4p^5(^3P)5p$ final states, respectively, over the $3d_{5/2} \rightarrow 5p, 6p$ and $3d_{3/2} \rightarrow 5p$ resonances. Figures 5 and 6 contain the corresponding results for the 4*p* main-line cross section and asymmetry parameter. The spectator-satellite cross sections were scaled to the 4*p* cross section, which itself was scaled to absorption²⁰ at 89.9 eV after consideration of the intensities of the 4*s* main line (from Fig. 1), the valence-shell correlation satellites,²¹ and valence double ionization²² at this photon energy. The spectator transitions had no appreciable intensity at 89.9 eV.

The data in Figs. 2–4 and 6 were fitted to three Lorentzian profiles convoluted with a Gaussian function of 0.10 eV full width at half maximum (FWHM) to account for the finite monochromator resolution. The natural linewidth was taken to be 0.11 eV.⁵ Although a Lorentzian lineshape is not strictly correct for an asymmetry parameter,²³ it was sufficient to fit the β_{4p} data adequately. The 4*p* cross-section data were fitted with three Fano profiles,²⁴ also convoluted with a Gaussian function as above. Due to the poor quality of the σ_{4p} data, we consider this fit just an illustration of the asymmetry of the 4*p* cross-section profiles for these three resonances, and thus we do not report Fano parameters. The 4*s* cross section and asymmetry parameter also were measured in this experiment, and were found to be unaffected by the $3d \rightarrow np$ resonances.

The resonant enhancement of the spectator satellites in Figs. 2–4 are fitted well by Lorentzian profiles. This implies that no significant autoionization interference is occurring in these decay channels, as one expects because there is little off-resonance intensity for these peaks. The nonresonant background intensity for peak 1a in Fig. 2 comes mostly from second-order $M_{4,5}N_{2,3}N_{2,3}$ Auger decay. The relative $3d_{5/2}/3d_{3/2}$ spin-orbit intensities for the peaks 1a, 1, and 2 in Figs. 2–4 vary slightly from one spectator satellite to another. We attribute this to the fact that these peaks contain multiple configurations that may be affected differently at the $3d_{5/2}$ or $3d_{3/2}$ resonances. The influence of the $3d_{5/2} \rightarrow 6p$ resonance also may be important.

The larger width of the $3d_{3/2} \rightarrow 5p$ profile for peak 1a compared to that for peaks 1 or 2 is likely due to the $3d_{5/2} \rightarrow 6p$ resonance, which would enhance the $4p^4 6p$ configurations that are included in peak 1a. Peaks 1 and 2 do not contain configurations with a 6*p* electron,⁷ so they should not be enhanced as much at the $3d_{5/2} \rightarrow 6p$ excitation. Finally, the high points above 93 eV in the peak 1a cross section result from $3d_{5/2} \rightarrow 7p$ and higher

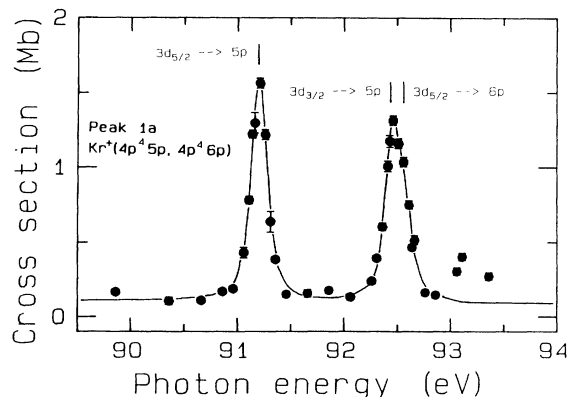


FIG. 2. Partial cross section of peak 1a ($4p^4 5p$ and $4p^4 6p$) in the Kr $3d \rightarrow np$ region. The off-resonance intensity for this peak is due to $\text{Kr}^+ (3d^{-1}) M_{4,5}N_{2,3}N_{2,3}$ Auger decay induced by second-order radiation (see bottom spectrum of Fig. 1). The solid curve is a fit with three Lorentzian functions (FWHM, 0.11 eV, Ref. 5) convoluted with a Gaussian of 0.10-eV FWHM. High points above 93 eV are explained in the text.

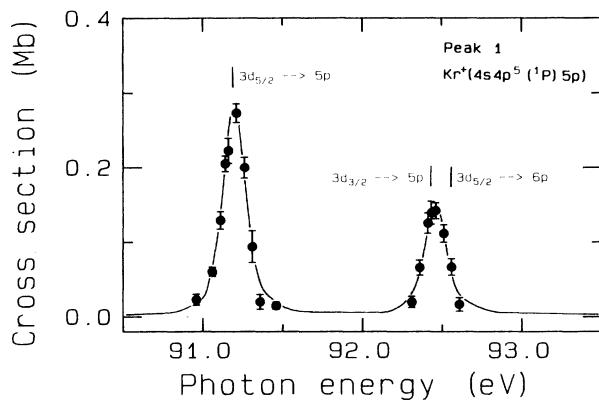


FIG. 3. Partial cross section of peak 1 [$4s4p^5(^1P)5p$] as in Fig. 2. At off-resonance photon energies for which data is shown in Fig. 2, peak 1 had no measurable intensity, and thus no points are shown.

np resonances, which presumably can decay to $4p^47p$, etc. final states that are included in peak 1a.

The $4p$ cross-section results in Fig. 5 exhibit only about a 10% effect at the $3d \rightarrow 5p$ resonances. The resonant effect at the $3d_{5/2} \rightarrow 6p$ resonance was difficult to fit, but was much smaller than the effect for the $5p$ excitations. The differential effect on σ_{4p} accounts for only 2% of the total decay to Kr^+ for the $3d_{5/2} \rightarrow 5p$ resonance (see Table I). However, the asymmetric profiles in σ_{4p} show that coupling of the $4p$ continua to the $3d \rightarrow 5p$ resonances is significant.

More pronounced effects occur for the $4p$ asymmetry parameter shown in Fig. 6. Here we see changes of $+0.5$ in β_{4p} , which can be a parameter more sensitive to the coupling of continuum channels with an autoionization resonance. An intriguing observation for β_{4p} is that the $3d_{5/2} \rightarrow 6p$ resonance appears to have a significant influence on the asymmetry parameter, broadening the β_{4p} peak at 92.5 eV. This result can be discerned best by comparing the widths of the features at 91.2 and 92.5 eV in Fig. 6. We offer no explanation for this result.

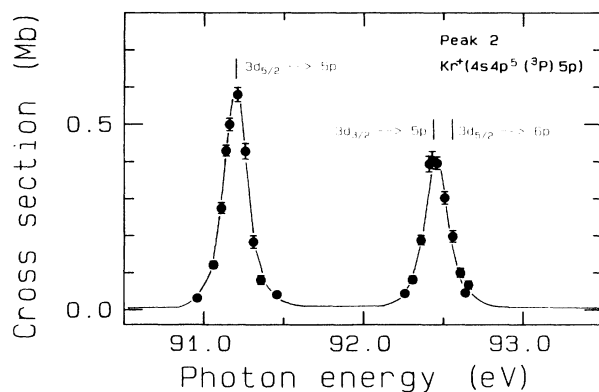


FIG. 4. Partial cross section of peak 2 [$4s4p^5(^3P)5p$] as in Figs. 2 and 3.

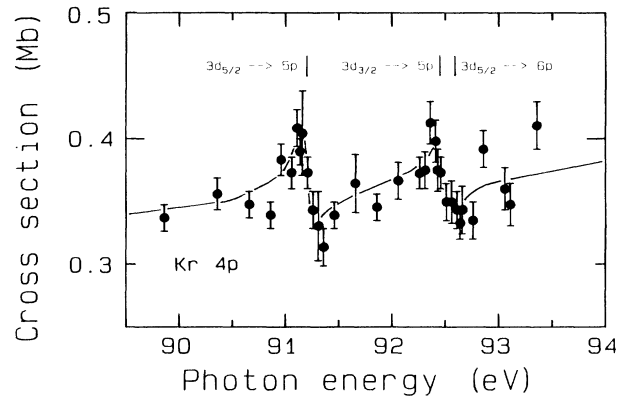


FIG. 5. Partial cross section of the $4p$ main line in the vicinity of the Kr $3d \rightarrow np$ resonances. The data were scaled to absorption (Ref. 19) at 89.9 eV as described in the text. The curve is a fit to the data with three Fano functions (FWHM, 0.11 eV, Ref. 5) convoluted with a Gaussian of 0.10-eV FWHM.

Despite the importance of spectator satellites to the decay of the Kr $3d \rightarrow 5p, 6p$ resonances, the σ_{4p} and β_{4p} results illustrate that the spectator model (i.e., Auger-like decay of the core hole) is not the whole story. In general, the spectator model should yield a reasonably accurate estimate of the identities of the resonantly enhanced features in inner-shell resonant photoelectron spectra, but it omits the possible effects of autoionization on the main-line features, in this case on $Kr^+ 4p^{-1}$ which are clearly observed. Also important to the resonant decay is the possibility of shake-up or shake-off of the initially excited electron in the decay process. These effects occur in normal Auger spectra, and we have observed both shake-up in the present results and shake-off in threshold-electron spectroscopy of the Kr $3d$ resonances.¹⁰

IV. CONCLUSIONS

High-photon-resolution resonant photoelectron spectra of Kr have been recorded in the vicinity of the $3d_{5/2} \rightarrow 5p, 6p$ and $3d_{3/2} \rightarrow 5p$ autoionizing resonances.

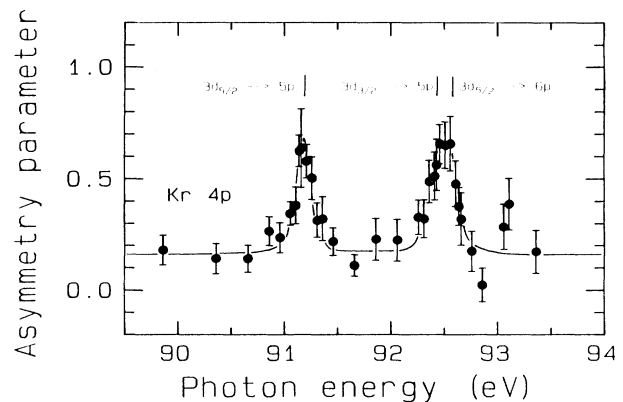


FIG. 6. Asymmetry parameter of the $4p$ main line, fit in the same manner as in Fig. 2.

The results agree well with previous lower-photon-resolution measurements. The photoemission features enhanced on these resonances are similar to those seen in $\text{Kr}^+ M_{4,5}NV$ Auger spectra, except that the final states observed in the resonant spectra contain a $5p$ (or higher np) electron. Comparison of photoemission spectra on the different resonances has allowed new assignments of some of the spectator-satellite features; in particular, final states containing a $6p$ or $7p$ electron have been better identified. Resonance profiles have been measured for cross sections for some of the resonantly enhanced satellites and for the $4p$ cross section and angular distribution. All of these results illustrate the dominance of spectator Auger-like decay of the $3d$ hole in the excited state, but

also show the importance of coupling to the nonspectator $4p^{-1}$ channels.

ACKNOWLEDGMENTS

We thank C. E. Brion for helpful discussions. This work was supported by the Director, Office of Energy Research, Office of Basic Energy Sciences, Chemical Sciences Division of the U.S. Department of Energy under Contract No. DE-AC03-76SF00098. It was performed at the Stanford Synchrotron Radiation Laboratory, which is supported by the Department of Energy's Office of Basic Energy Sciences. One of us (M.N.P.) acknowledges support from the Fulbright Foundation.

*Present address: National Bureau of Standards, Gaithersburg, MD 20899.

†Permanent address: Department of Chemistry, University of Rome "La Sapienza," 00100 Rome, Italy.

¹W. Eberhardt, G. Kalkoffen, and C. Kunz, *Phys. Rev. Lett.* **41**, 156 (1978).

²M. Y. Adam, F. Wulleumier, N. Sandner, S. Krummacher, V. Schmidt, and W. Mehlhorn, *Jpn. J. Appl. Phys.* **17**, 170 (1978).

³V. Schmidt, *Appl. Opt.* **19**, 4080 (1980).

⁴S. Southworth, U. Becker, C. M. Truesdale, P. H. Kobrin, D. W. Lindle, S. Owaki, and D. A. Shirley, *Phys. Rev. A* **28**, 261 (1983).

⁵T. Hayaishi, Y. Morioka, Y. Kageyama, M. Watanabe, I. H. Suzuki, A. Mikuni, G. Isoyama, S. Asaoka, and M. Nakamura, *J. Phys. B* **17**, 3511 (1984).

⁶H. Aksela, S. Aksela, G. M. Bancroft, K. H. Tan, and H. Pulkkinen, *Phys. Rev. A* **33**, 3867 (1986).

⁷H. Aksela, S. Aksela, H. Pulkkinen, G. M. Bancroft, and K. H. Tan, *Phys. Rev. A* **33**, 3876 (1986).

⁸U. Becker, T. Prescher, E. Schmidt, B. Sonntag, and H.-E. Wetzal, *Phys. Rev. A* **33**, 3891 (1986).

⁹U. Becker, H. G. Kerkhoff, D. W. Lindle, P. H. Kobrin, T. A. Ferrett, P. A. Heimann, C. M. Truesdale, and D. A. Shirley, *Phys. Rev. A* **34**, 2858 (1986).

¹⁰P. A. Heimann, U. Becker, H. G. Kerkhoff, B. Langer, D. Szostak, R. Wehlitz, D. W. Lindle, T. A. Ferrett, and D. A. Shirley, *Phys. Rev. A* **34**, 3782 (1986).

¹¹L. O. Werme, T. Bergmark, and K. Siegbahn, *Phys. Scr.* **6**, 141 (1972).

¹²W. Mehlhorn, W. Schmitz, and D. Stalherm, *Z. Phys.* **252**, 399 (1972).

¹³H. Aksela, S. Aksela, and H. Pulkkinen, *Phys. Rev. A* **30**, 2456 (1984).

¹⁴M. G. White, R. A. Rosenberg, G. Gabor, E. D. Poliakoff, G. Thornton, S. H. Southworth, and D. A. Shirley, *Rev. Sci. Instrum.* **50**, 1288 (1979).

¹⁵D. W. Lindle, T. A. Ferrett, U. Becker, P. H. Kobrin, C. M. Truesdale, H. G. Kerkhoff, and D. A. Shirley, *Phys. Rev. A* **31**, 714 (1985).

¹⁶D. W. Lindle, P. A. Heimann, T. A. Ferrett, P. H. Kobrin, C. M. Truesdale, U. Becker, H. G. Kerkhoff, and D. A. Shirley, *Phys. Rev. A* **33**, 319 (1986).

¹⁷C. N. Yang, *Phys. Rev.* **74**, 764 (1948).

¹⁸G. C. King, M. Tronc, F. H. Read, and R. C. Bradford, *J. Phys. B* **10**, 2479 (1977); G. C. King and F. H. Read, in *Atomic Inner-Shell Physics*, edited by B. Crasemann (Plenum, New York, 1985), p. 317.

¹⁹V. Schmidt, S. Krummacher, F. Wulleumier, and P. Dhez, *Phys. Rev. A* **24**, 1803 (1981).

²⁰G. V. Marr and J. B. West, *At. Data Nucl. Data Tables* **18**, 497 (1976).

²¹Estimated from Ar valence satellite intensities; see M. Y. Adam, F. Wulleumier, S. Krummacher, V. Schmidt, and W. Mehlhorn, *J. Phys. B* **11**, L413 (1978).

²²J. A. R. Samson and G. N. Haddad, *Phys. Rev. Lett.* **33**, 875 (1974); Th.M. El-Sherbini and M. J. van der Wiel, *Physica (Utrecht)* **62**, 119 (1972).

²³N. M. Kabachnik and I. P. Sazhina, *J. Phys. B* **9**, 1681 (1976).

²⁴U. Fano, *Phys. Rev.* **124**, 1866 (1961).